In-Line Signal Circuit for Broad-Band Parametric Amplifiers

SHUNICHIRO EGAMI, MEMBER, IEEE

Abstract—**A new double-tuned parametric amplifier signal-circuit configuration and a method for its experimental optimization is described. A new in-line signal circuit, which is adapted from a quarter-wave-coupled bandpass filter, is intended for use at higher microwave and millimeter-wave parametric amplifiers (paramps). It is shown that, using this signal circuit, a broader flat-gain response can be obtained as compared with the conventional double-tuned signal circuit with broad-banding stub placed multihalf-wavelength apart from the diode. To suppress the spurious response, a semi-lumped approximation is applied in the design. Finally, a "cold and hot" test method to optimize the double-tuned signal circuit is introduced.**

I. INTRODUCTION

BECAUSE of solid-state pumping and low-noise room-temperature operation, the microwave parametric amplifier (paramp) has become a simple but very useful device in recent years. In addition, its realizable bandwidth has been considerably increased by use of signal-circuit broad-banding techniques and high performance varactor diodes.

However, design of upper microwave and millimeter-wave paramps have not been fully exploited, hence their realizable fractional bandwidth has been small compared with that of the lower microwave paramps [1]–[5].

It is well known that, by including a second resonator in the signal circuit, a broad flat gain can be obtained. This signal-circuit double-tuning resonator is essential in realizing a broad flat-gain response, because its positive slope parameter provides a large measure of cancellation effect of the negative susceptance slope parameter [6] associated with the pumped diode, and triple tuning or higher orders of broadbanding do not yield as large an increase in flat-gain bandwidth as compared with double tuning.

Although the design theory of double-tuned paramps has been exploited [6]–[11], some difficulties have been experienced in the physical realization of the double-tuned signal circuit, especially at upper microwave and millimeter-wave frequencies.

This paper describes a new type of double-tuned signal circuit adapted from a quarter-wave-coupled bandpass filter (BPF), which is easy to design even at upper microwave and millimeter-wave frequencies, and has distinctive advantages compared with the conventional double-tuned signal circuit incorporating a half-wavelength open-ended stub [2].

Manuscript received April 18, 1974; revised September 9, 1974.
The author is with the Electrical Communication Laboratories, Nippon Telegraph and Telephone Public Corporation, Yokosuka-shi, Japan.

II. NORMALIZED SLOPE PARAMETERS AND THEIR RELATIONSHIP TO GAIN-FREQUENCY RESPONSE

Lead inductance L_s, mean elastance (inverse of capacitance) S_0, and series resistance R_s of the pumped varactor diode are common elements in both the signal and the idler resonant circuits. Therefore, although it is desired to lower the slope parameter of each resonant circuit as possible, they are restricted by the slope parameter associated with the varactor diode itself. Accordingly, in the previous paper [6], slope parameter of each resonant circuit is normalized by the slope parameter associated with the diode itself as

$$a_1 = x_1/x_{10} \tag{1}$$

$$a_2 = x_2/x_{20} \tag{2}$$

where

x_1	reactance slope parameter of the signal resonant circuit;	
$x_{10} = \omega_{10}L_s$	slope parameter associated with the diode at signal center frequency ω_{10};	(3)
x_2	reactance slope parameter of the idler resonant circuit;	
$x_{20} = \omega_{20}L_s$	slope parameter associated with the diode at idler center frequency ω_{20}.	(4)

These normalized slope parameters, which are always greater than unity, can be approximately estimated from the signal and idler equivalent circuits.

Fig. 1 shows the signal frequency equivalent circuit of the double-tuned paramps. Negative resistance $-R_a$ and negative susceptance slope parameter $-b_a$ represent the contribution of the idler resonant circuit at signal frequency. They are given as [6],

$$R_a = \tilde{Q}_1\tilde{Q}_2R_s \tag{5}$$

$$b_a = a_2x_{10}/\tilde{Q}_1\tilde{Q}_2R_s^2 \tag{6}$$

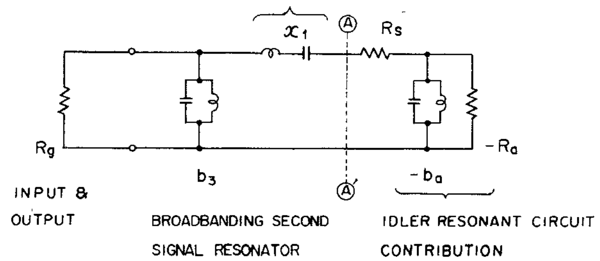

Fig. 1. Double-tuned paramp signal frequency equivalent circuit.

where $\tilde{Q}_1$ and $\tilde{Q}_2$ are the dynamic Q of the varactor diode at the signal and idler frequencies, which are defined by $\tilde{Q}_1 = S_1/(\omega_{10}R_s)$, $\tilde{Q}_2 = S_1/(\omega_{20}R_s)$, when elastance of pumped varactor is expanded at pump frequency ω_p as, $S = S_0 + 2S_1 \cos \omega_p t + \cdots$.

As shown in the previous paper [6], the paramps exhibit positive gain at the frequency where the impedance of the right-hand circuit of Ⓐ Ⓐ′ in Fig. 1 has negative real part, which is satisfied in the fractional bandwidth (normalized to ω_{10}) of

$$\Omega_0 = R_s(\tilde{Q}_1\tilde{Q}_2 - 1)^{1/2}/(a_1 x_{10}). \tag{7}$$

This "active" fractional bandwidth is independent on the value of R_g and b_3, thus it is not affected by paramp midband gain level and degree of double tuning. However, by the virtue of double tuning, a broad flat-gain response can be formed over this constant "active" bandwidth.

This broadbanding can be considered due to the cancellation of negative slope parameter $-b_a$ by positive slope parameter b_3. Therefore, degree of cancellation depends on the relative magnitude of the signal resonant circuit slope parameter x_1, which exists between $-b_a$ and b_3. That is, if the effect of x_1 is relatively small compared with the effect of $-b_a$, a broad flat-gain bandwidth approaching the positive-gain bandwidth can be obtained by making $b_3 \approx b_a$.

This flat-bandwidth capability is actually closely related to the value of a_1/a_2 ($=Q$ of signal resonant circuit $x_1 R_s^{-1}/Q$ of idler circuit contribution $b_a R_a$).

In Fig. 2, flat-bandwidth capability (Ω_A/Ω_0, Ω_A; fractional bandwidth normalized to ω_{10}, in which stipulated gain and ripple are attained) is represented as a function of a_1/a_2. Although these curves are also dependent on the value of $\tilde{Q}_1\tilde{Q}_2$, this dependence is very small if $\tilde{Q}_1\tilde{Q}_2$ is sufficiently greater than 1, as is the case for almost every paramp.

As a result, it is seen therein that to obtain a broad flat-gain response, it is necessary to achieve 1) greater positive-gain "active" fractional bandwidth, and 2) greater flat-bandwidth capability Ω_A/Ω_0. The first condition is dependent on the modulation factor of the diode and idler circuit normalized slope parameter a_2 [6], and the second condition, which is the concern of this paper, is dependent mostly on the signal resonant circuit normalized slope parameter a_1.

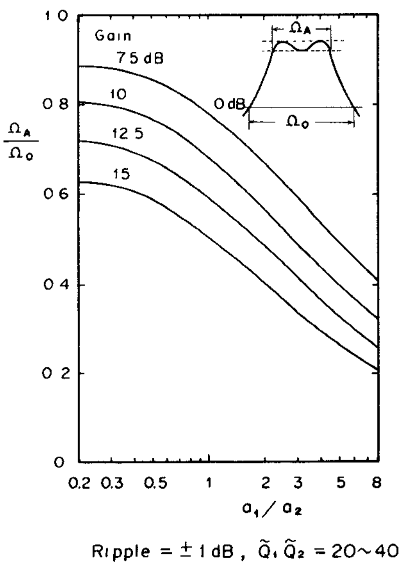

Fig. 2. Achievable flat-gain bandwidth normalized to positive-gain bandwidth versus a_1/a_2.

III. EFFECT OF BROAD-BANDING SIGNAL RESONATOR LOCATION

As shown in the preceding section, a lower value of a_1/a_2 gives a greater flat-bandwidth capability. This condition can be attained by reducing the value of a_1, since a_2 is made as small as possible to get a greater Ω_0.

In the past, the second signal resonator was usually realized by a half-wavelength open-ended stub, placed one or two half-wavelengths from the diode [2]. However, as shown in Fig. 3, this multihalf-wavelength spacing, which can be represented by equivalent series resonant circuit with slope parameter x_{1s}, directly increases the total signal resonant circuit slope parameter x_1.

If the characteristic impedance of this multihalf-wavelengths line is assumed equal to the required source impedance R_g and the line length is represented as $n\lambda_{10}/2$, ($n = 1,2,\cdots$, λ_{10}; signal center frequency wavelength), slope parameter x_{1s} is approximately given by the following equation:

$$x_{1s} = \frac{n\pi}{2} R_a \left(\frac{R_g}{R_a} - \frac{R_a}{R_g}\right). \tag{8}$$

For a 19-GHz paramp, as described in a following section, typical values are, $R_a \approx 50\ \Omega$, $R_g/R_a \approx 1.8$ (corresponds to 10-dB gain), $x_{10} \approx 45\ \Omega$ then, if increase of a_1 is represented by a_{1s}, it is given approximately as

$$a_{1s}(=x_{1s}/x_{10}) \approx 2.2n. \tag{9}$$

Thus even one or two half-wavelength lines between the diode and the second signal resonator increase the value of a_1 considerably, degrading the flat-bandwidth capability of a double-tuned paramp.

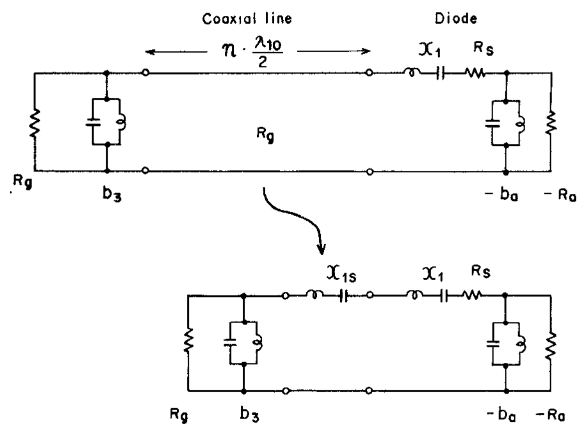

Fig. 3. Increase in signal resonant circuit slope parameter x_1 due to multihalf-wavelengths line between the second signal resonator and diode.

IV. A NEW TYPE DOUBLE-TUNED SIGNAL CIRCUIT

The design and adjustment of the signal circuit are most important in paramp realization, because the shape of the gain response is established by this circuit. For satisfactory paramp operation, the signal circuit must perform the following functions:

1) transformation of the external source impedance for the desired gain level;
2) double tuning to obtain a broad flat-gain response;
3) suppression of idler and pump power leakage to the signal path.

Here a new type in-line signal circuit which satisfies conditions 1) and 2) is presented. A design approach through which condition 3) is satisfied will be described in the next section.

A half-wavelength high-impedance line connected at both ends to a quarter-wavelength low-impedance line, which corresponds to one section of a quarter-wave-coupled BPF, is equivalently represented by a parallel resonant circuit, as shown in Fig. 4.

In the figure, b_3 is the slope parameter of the parallel resonant circuit, and $x_{3s}/2$ is the parasitic series resonant circuit slope parameter associated with it.

Using this parallel resonant circuit as the second signal resonator, the previously described increase in signal resonant circuit slope parameter can be greatly reduced, because, in this circuit the second signal resonator is placed as near the diode as possible. In addition, proper choice of the quarter-wavelength line characteristic impedances yields the required transformation of the external source impedance to the desired source impedance.

These are given by the following approximate equations

$$b_3 = (\pi/4K_{01}^2)(K_{01} + K_{12} + 2Z_1) \quad (10)$$

$$\frac{x_{3s}}{2} = \frac{\pi K_{12}^4}{8K_{01}^2}\left(\frac{1}{K_{01}} + \frac{1}{K_{12}} + \frac{2}{Z_1}\right) \quad (11)$$

$$R_g/R_0 = K_{01}^2/K_{12}^2 \quad (12)$$

where K_{01}, K_{12}, and Z_1 are characteristic impedances of each section, as shown in the figure.

In this signal circuit, increase in the signal resonant circuit slope parameter can be considered as $x_{3s}/2$. Therefore, the corresponding increase in a_1 is given by

$$a_{1s} = x_{3s}/(2x_{10}). \quad (13)$$

In most cases, this is much smaller than the corresponding value for the signal circuit utilizing a half-wavelength open-ended stub described in a preceding section. For example, in the case of 19-GHz paramps, as described in a later section, typical values are $K_{01} \approx K_{12} \approx 20\ \Omega$, $Z_1 \approx 70\ \Omega$, $x_{10} \approx 45\ \Omega$. This yields a value of a_{1s} as 0.4, which results in reduced value of a_1 and in a larger flat-bandwidth capability.

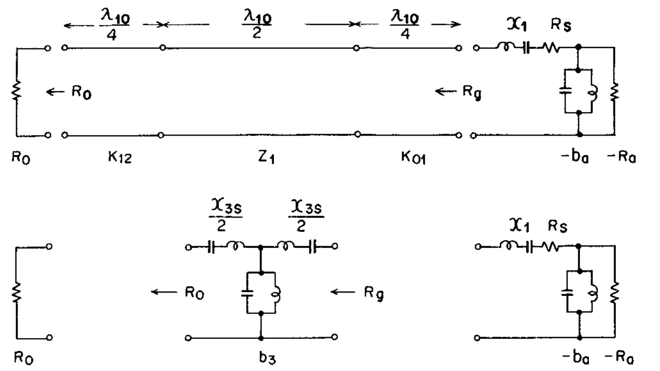

Fig. 4. In-line-type double-tuned signal circuit and its equivalent circuit. b_3 is the slope parameter of the parallel resonant circuit which corresponds to the second signal resonator. $x_{3s}/2$ is the parasitic reactance slope parameter which represents the increase of the signal resonant circuit slope parameter.

V. SPURIOUS FREE SEMILUMPED SIGNAL-CIRCUIT DESIGN

The signal circuit shown in Fig. 4, consisting of alternate quarter-, half-, quarter-wavelength sections of coaxial line, exhibits spurious responses at multiples of the signal frequency. In most cases, these spurious responses result in leakage of idler or pump power into the input signal circuit, thus making it inapplicable to the paramp.

However, these spurious responses can be suppressed by replacing the distributed constant line by a quasi-lumped constant low-pass filter (LPF) having the same signal frequency transmission characteristics.

For example, a constant-K-type LPF [12], with image impedance Z_0 and a phase shift 90°, is equivalent to a quarter-wavelength coaxial line with characteristic impedance Z_0.

Fig. 5 shows the transmission characteristic of the 180° phase shift constant-K LPF and quasi-lumped constant coaxial LPF which approximate the lumped constant LPF.

Fig. 5(a) shows the transmission characteristics of the 180° phase shift constant-K LPF with an image impedance of 50 Ω. Fig. 5(b) and (c) show the computer simulated transmission characteristics of the quasi-lumped coaxial circuit which approximates the lumped constant LPF at 18.5 GHz.

The coaxial circuit (b) approximates the lumped constant LPF (a) more closely than (c) because the characteristic impedance of the low-impedance section in (b) is lower than that in (c), which makes the low-impedance section in (b) shorter, thus making it more closely resemble a lumped constant network. Therefore, in the design, it is advantageous to realize the capacitances by the lower impedance sections and the inductances by the higher impedance sections, although this is limited by the difficulty of the fabrication.

This approach is applied in the design of the in-line signal circuit described in a preceding section. In Figs. 6 and 7, the design procedure and computer simulated transmission characteristics for a 19-GHz paramp in-line signal circuit are depicted.

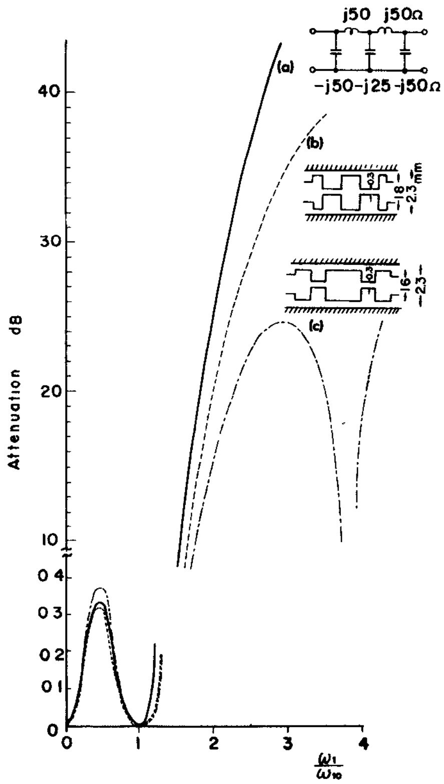

Fig. 5. Computer simulated transmission characteristics of quasi-lumped constant approximation of a half-wavelength 50-Ω line. (a) 180° phase shift, constant-K LPF with image impedance of 50 Ω. (b) Realization of (a) by the coaxial line. Alternate high- and low-impedance coaxial line sections have characteristic impedance of 122 Ω and 15 Ω, respectively. (c) The same as (b), except characteristic impedance of the low-impedance section is chosen as 22 Ω. Design frequency ω_{10} is 18.5 GHz. These coaxial LPF's are free of higher order mode propagation at frequencies ω_1 below 73 GHz.

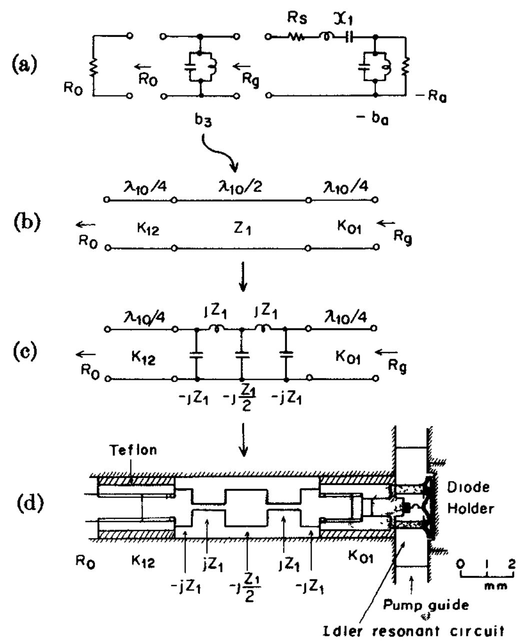

Fig. 6. Design evolution of quasi-lumped in-line double-tuned signal circuit. (a) Equivalent circuit of double-tuned signal circuit. (b) Realization of signal circuit by a quarter-wave-coupled BPF. (c) Quasi-lumped approximation of half-wavelength resonator. (d) Realization of quasi-lumped coaxial LPF, comprising 19-GHz paramp signal circuit.

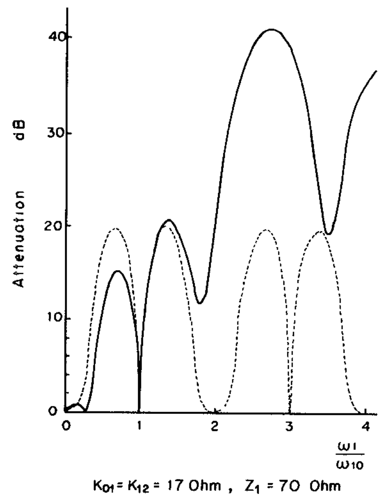

Fig. 7. Calculated transmission characteristic of quasi-lumped in-line signal circuit shown in Fig. 6(d) (solid line). Dotted line shows the transmission characteristic when quasi-lumped approximation is not applied. ω_1/ω_{10} signal frequency normalized to signal center frequency.

In the design, the half-wavelength high-impedance line is approximated by a 180° phase shift constant-K LPF. Then this lumped constant LPF is approximated by the coaxial structure. For the quarter-wavelength low-impedance sections, the lumped constant approximation is not applied because these sections must also serve, respectively, as the diode contacting mechanism and the connection to the input coaxial line.

Low-impedance sections K_{01}, K_{12} and high-impedance section Z_1 are fabricated individually and threaded for direct interconnection, thus simplifying the experimental optimization.

In this circuit, idler or pump power is rejected by the high-impedance LPF section. The effect of the quarter-wavelength low-impedance section on these frequencies can be considered small, because the characteristic impedance of the quarter-wavelength line is low, compared with the idler or pump guide characteristic impedance.

VI. EXPERIMENTAL SIGNAL CIRCUIT OPTIMIZATION TECHNIQUE

The optimum slope parameter of the second signal resonator is closely related to the negative slope parameter of the diode [6].

Although the value of b_a, which is formulated in (6), can be estimated for a given varactor diode and idler circuit, the actual value generally differs somewhat from it. Therefore, in most cases, slope parameter b_3 of the second signal resonator must be experimentally optimized.

Here a new "cold and hot" test method, which facilitates the experimental optimization of b_3, is described.

When the pump power is off, the equivalent circuit of the double-tuned paramp can be represented as shown in Fig. 8(a). Since the series and parallel resonant circuits which are characterized by x_1 and b_3 are each resonant at ω_{10}, this equivalent circuit can be considered as two-section BPF with termination impedances R_g and R_s.

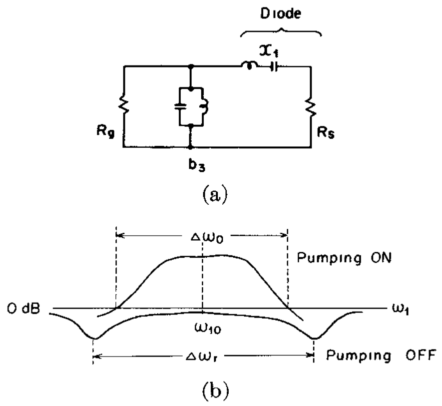

Fig. 8. (a) Unpumped double-tuned paramp equivalent circuit. (b) Pumped paramp gain and unpumped loss.

Therefore, in the pump off condition the return loss has two negative peaks equally separated from the signal center frequency, as shown in Fig. 8(b).

If the frequency separation between these negative peaks is represented by $\Delta\omega_r$, $\Delta\omega_r/\omega_{10}$ can be calculated from the equivalent circuit as

$$\frac{\Delta\omega_r}{\omega_{10}} = \frac{R_s}{x_{10}} (a_1 a_2 \eta \beta)^{-1/2} \left\{ \frac{\beta}{\alpha} - \frac{1}{2}\left(q + \frac{1}{q}\right)\right\}^{1/2} \tag{14}$$

where

$$\eta = b_3/b_a, \qquad \alpha = R_s/R_a, \qquad \beta = R_g/R_a,$$
$$q = Q_3/Q_1 \; (Q_1 = x_1/R_s, \; Q_3 = b_3 R_g).$$

Since, in most cases,

$$\beta/\alpha \gg 1, \qquad q \approx 1$$

the preceding equation can be approximately represented as

$$\Delta\omega_r/\omega_{10} = (R_s/x_{10})(a_1 a_2 \eta \alpha)^{-1/2}. \tag{15}$$

On the other hand, under the pumped condition, paramps have a positive-gain fractional bandwidth $\Omega_0[= \Delta\omega_0/\omega_{10}$ in Fig. 8(b)], which is given in (7). This can be approximately represented for $\tilde{Q}_1\tilde{Q}_2 \gg 1$ as

$$\frac{\Delta\omega_0}{\omega_{10}} = \frac{R_s}{x_{10}} \frac{\alpha^{-1/2}}{a_2}. \tag{16}$$

Then using the preceding relations, $\Delta\omega_0/\Delta\omega_r$ is given as

$$\frac{\Delta\omega_0}{\Delta\omega_r} = \left(\frac{a_1}{a_2}\eta\right)^{1/2}. \tag{17}$$

Since a_1/a_2 can be roughly estimated by the signal and idler equivalent circuit, the preceding equation gives the relation between $\eta(= b_3/b_a)$ and $\Delta\omega_0/\Delta\omega_r$. Thus there exists an optimum $\Delta\omega_0/\Delta\omega_r$ corresponding to the optimum η which is given by the design table [6]. In addition, η has a maximum limit for stable amplification represented by η_s, which is about $1.2 \sim 1.3$ times greater than optimum η [6]. Therefore, for stable amplification, the experimental ratio $\Delta\omega_0/\Delta\omega_r$ must satisfy the following equation:

$$\frac{\Delta\omega_0}{\Delta\omega_r} < \left(\frac{a_1}{a_2}\eta_s\right)^{1/2}. \tag{18}$$

VII. EXPERIMENTAL RESULTS

An experimental 19-GHz paramp with a new type in-line signal circuit is shown in Fig. 9.

The outer diameter of the coaxial line is chosen to be 2.3 mm so as not to allow higher order propagation of idler and pump ($54 \sim 57$ GHz) power. In this dimension, theoretical Q of the quasi-lumped high-impedance section is about 400 for typical design, about one third of straight coaxial line of the same characteristic impedance, thus it yields theoretical insertion loss of 0.2 dB (including a quarter-wavelength low-impedance section loss and assuming loaded Q of about 18), which was coincided with experimental result. The idler resonant circuit is formed by the diode and idler waveguide which is orthogonal to the pump guide as shown in Fig. 9.

Based upon the computer simulation on the equivalent circuit and also on experimental data, the value of a_2 is estimated as about 1.5, considering increase of idler resonant circuit resistance [6].

Waveguide–coaxial transition, which is indispensable in this frequency range, is deliberately designed for a broad operational bandwidth. The design shown in the figure exhibited a return loss higher than 17 dB over the 15–22-GHz frequency range.

The experimental paramp utilizes a GaAs planar p-n junction varactor packaged in a micro-pill-type structure formed by a thin Forsterite ($MgO\ SiO_2$) ring with small stray shunt capacitance (0.08 pF) and with typical parameter values $L_s = 0.4$ nH, $R_s = 2.5\ \Omega$, $C_{j0} = 0.15$ pF, and $\tilde{Q}_1 = 6$.

Fig. 10 shows the initial experimental gain response. Although an inexplicable spike in gain response appeared in the last case, upon variation of b_3 by changing the com-

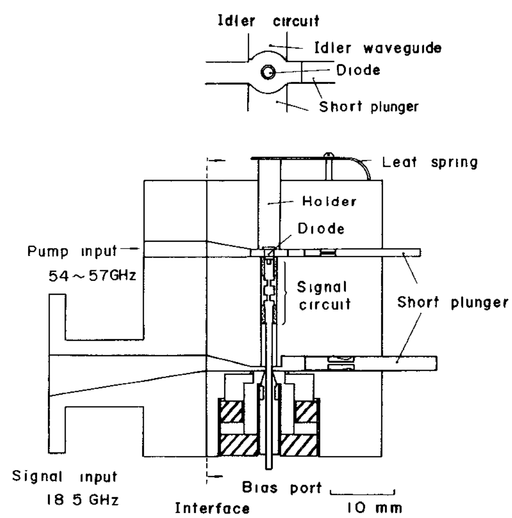

Fig. 9. Experimental 19-GHz double-tuned paramp.

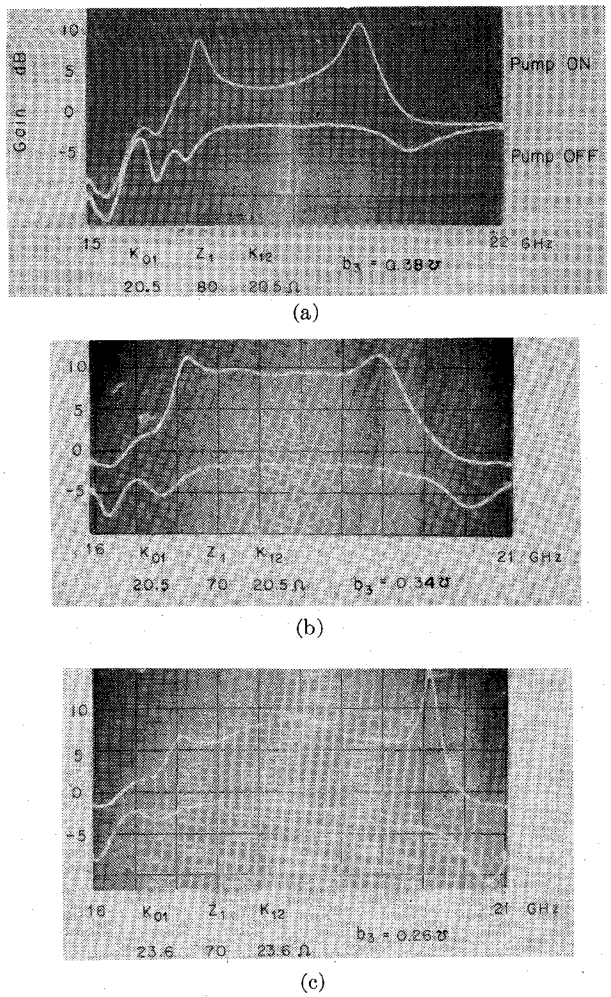

Fig. 10. Experimental paramp gain response as a function of b_3.

bination of K_{01}, Z_1, and K_{12}, the optimum flat-gain response is obtained for $b_3 = 0.34$ ℧, which is not so different from the calculated value of $b_3(\approx 0.7\ b_a) \approx 0.42$ ℧.

Obtained typical characteristics are a 10-dB-gain flat bandwidth of 2.4 GHz, positive-gain bandwidth of $4 \sim 4.5$ GHz, noise figure of 3.5 dB (band center), and 4.5 dB (band edge) including circulator loss 0.4 dB.

The ratio of the measured flat bandwidth to the positive-gain bandwidth Ω_A/Ω_0 is about 0.6, indicating that a_1/a_2 is near unity and that a_1 is reduced by the new signal circuit. Also in the figure, the position of the negative peaks in the unpumped gain response follows the variations in the second signal resonator slope parameter.

VIII. CONCLUSION

The bandwidth for positive gain is a fundamental measure of paramp bandwidth capability. However, the ratio of the flat-gain bandwidth to the positive-gain bandwidth is also an important parameter which determines the realizable flat-gain bandwidth.

It is shown that to achieve a greater flat-gain bandwidth, a smaller signal resonant circuit slope parameter is necessary. In connection to this effect, it is shown that even a half-wavelength line between the signal resonator and the diode results in degradation of the flat-gain bandwidth capability of the double-tuned paramp. To reduce this effect, and to facilitate signal-circuit design in millimeter-wave frequencies, a new in-line-type signal-circuit design approach was described. A practical spurious free design approach and simple experimental optimization method were also presented, along with results on an experimental 19-GHz paramp.

ACKNOWLEDGMENT

The author wishes to thank Dr. T. Okajima for helpful discussions and guidance through the course of this work, and also wishes to thank K. Misada for invaluable assistance in the experiments.

REFERENCES

[1] T. Okajima, M. Kudo, K. Shirahata, and D. Taketomi, "18-GHz paramps with triple-tuned gain characteristics for both room- and liquid-helium-temperature operation," *IEEE Trans. Microwave Theory Tech. (1972 Symposium Issue)*, vol. MTT-20, pp. 812–819, Dec. 1972.
[2] N. Takahashi *et al.*, "K band cryogenically cooled wide band nondegenerate parametric amplifier," in *G-MTT Int. Symp. Dig.*, 1970, pp. 100–103.
[3] Y. Kinoshita and M. Maeda, "An 18-GHz double-tuned parametric amplifier," *IEEE Trans. Microwave Theory Tech. (1970 Symposium Issue)*, vol. MTT-18, pp. 1114–1119, Dec. 1970.
[4] C. L. Cuccia, "Ultralow-noise parametric amplifiers in communication satellite earth terminals," in *Advance in Microwaves*, vol. 7. New York: Academic, 1971.
[5] H. C. Okean and H. Weingart, "S-band integrated parametric amplifier having both flat gain and linear phase response," *IEEE Trans. Microwave Theory Tech. (1968 Symposium Issue)*, vol. MTT-16, pp. 1057–1059, Feb. 1968.
[6] S. Egami, "A design theory for wide-band parametric amplifiers," *IEEE Trans. Microwave Theory Tech.*, vol. MTT-22, pp. 119–125, Dec. 1974.
[7] J. T. Dejager, "Maximum bandwidth performance of a nondegenerate parametric amplifier with single-tuned idler circuit," *IEEE Trans. Microwave Theory Tech.*, vol. MTT-12, pp. 459–467, July 1964.
[8] W. P. Connors, "Maximally flat bandwidth of a nondegenerate parametric amplifier with double tuned signal circuit and single tuned circuit," *IEEE Trans. Microwave Theory Tech.* (Corresp.), vol. MTT-13, pp. 251–252, Mar. 1965.
[9] V. Porra and P. Somervuo, "Broadband matching of a parametric amplifier by using Fano's method," *IEEE Trans. Microwave Theory Tech.*, vol. MTT-16, pp. 880–882, Oct. 1968.
[10] W. J. Getsinger, "Prototypes for use in broadbanding reflection amplifiers," *IEEE Trans. Microwave Theory Tech.*, vol. MTT-11, pp. 486–497, Nov. 1963.
[11] G. L. Matthaei, "A study of the optimum design of wide-band parametric amplifiers and up-converters," *IRE Trans. Microwave Theory Tech.*, vol. MTT-9, pp. 23–38, Jan. 1961.
[12] G. L. Matthaei *et al.*, *Microwave Filters, Impedance Matching Networks and Coupling Structures.* New York: McGraw-Hill, 1964.
[13] G. R. Branner and S.-P. Chan, "A new technique for synthesis of broad-band parametric amplifiers," *IEEE Trans. Microwave Theory Tech.*, vol. MTT-21, pp. 437–444, July 1973.